

# The Violation of Stokes-Einstein Relation in Supercooled water

Sow-Hsin Chen<sup>\*†</sup>, Francesco Mallamace<sup>†‡</sup>, Chung-Yuan Mou<sup>§</sup>,  
Matteo Broccio<sup>†‡</sup>, Carmelo Corsaro<sup>‡</sup>, Antonio Faraone<sup>‡</sup>, and Li Liu<sup>†</sup>

<sup>†</sup>*Department of Nuclear Science and Engineering,*

*Massachusetts Institute of Technology, Cambridge MA 02139 USA*

<sup>‡</sup>*Dipartimento di Fisica and CNISM, Università di Messina I-98166, Messina, Italy and*

<sup>§</sup>*Department of Chemistry, National Taiwan University, Taipei, Taiwan*

(Dated: July 14, 2018)

By confining water in nanopores, so narrow that the liquid cannot freeze, it is possible to explore its properties well below its homogeneous nucleation temperature  $T_H \approx 235$  K. In particular, the dynamical parameters of water can be measured down to 180 K approaching the suggested glass transition temperature  $T_g \approx 165$  K. Here we present experimental evidence, obtained from Nuclear Magnetic Resonance and Quasi-Elastic Neutron Scattering spectroscopies, of a well defined decoupling of transport properties (the self-diffusion coefficient and the average translational relaxation time), which implies the breakdown of the Stokes-Einstein relation. We further show that such a non-monotonic decoupling reflects the characteristics of the recently observed dynamic crossover, at about 225 K, between the two dynamical behaviors known as fragile and strong, which is a consequence of a change in the hydrogen bond structure of liquid water.

PACS numbers: 61.20.Lc, 61.12.Ex, 64.70.Pf

Despite its fundamental importance in science and technology, the physical properties of water are far from being completely understood. The liquid state of water is unusual especially at low temperatures [1, 2, 3]. For example, contrary to other liquids, water behaves as if there exists a singular temperature toward which its thermodynamical properties, such as compressibility, thermal expansion coefficient, and specific heat, diverge [1]. The efforts of scientists from many disciplines to seek a coherent explanation for this unusual behavior, in combination with its wide range of impacts, make water one of the most important open questions in science today. On the other hand, the nature of the glass transition (GT) of water represents another challenging subject for current research [4]. Dynamical measurements in glass forming liquids have shown a dramatic slowdown of both macroscopic (viscosity  $\eta$  and self-diffusion coefficient  $D$ ) and microscopic (average translational correlation time  $\tau$ ) observables, as temperature is lowered towards the GT temperature  $T_g$ . Accordingly, a comprehension of the GT has been sought through the study of the dynamics at the molecular level, which, despite all efforts, has not yet been completely understood [5, 6, 7, 8]. Keeping in mind the “complexities” of both low-temperature water and its GT, we present here direct measurements of two dynamical parameters of water: the self-diffusion coefficient and the average translational relaxation time, in the temperature range from 280 to 190 K, obtained by Nuclear Magnetic Resonance (NMR) and Quasi-Elastic Neutron Scattering (QENS) experiments, respectively.

Bulk water can be supercooled below its melting temperature ( $T_M$ ) down to  $\approx 235$  K, below which it

inevitably crystallizes; it is just in such supercooled metastable state that the anomalies in its thermodynamical properties are most pronounced, showing a power law divergence towards a singular temperature  $T_S = 228$  K. At ambient pressure, water can exist in a glassy form below 135 K. Depending on  $T$  and  $P$ , glassy water has two amorphous phases with different structures: a low (LDA) and a high (HDA) density amorphous ice; thus it shows a polymorphism. LDA can be formed from HDA and vice versa; LDA, if heated, undergoes a glass-to-liquid transition transforming into a highly viscous fluid, then crystallizes into cubic ice at  $T_X \approx 150$  K. Thus an experimentally inaccessible  $T$  region exists in bulk water between  $T_H$  and  $T_X$ . Experiments performed within this interval could be of fundamental interest for understanding the many open questions on the physics of water. For example, the presence of a first order liquid-liquid transition line (LLTL), the precise location of its  $T_g$ , recently suggested at about 165 K [4, 9], and the existence of a *fragile-to-strong dynamic crossover* (FSC) on approaching  $T_g$  from the liquid side [10]. The existence of a LLTL leads to conjecture that liquid water possesses a low-temperature second critical point (predicted to be located at  $T_c \approx 220$  K,  $P_c \approx 1$  Kbar) [2], below which it can switch from one phase, a high density liquid (HDL), to another phase, a low density liquid (LDL), whose corresponding vitreous forms are the HDA and LDA, respectively. The difference between the two liquid phases lies in the water structure: in the HDL, the local tetrahedrally coordinated hydrogen-bond network is not fully developed, whereas in the LDL a more open, locally ice-like, hydrogen-bond network is fully developed [11]. Thus, near  $T_c$ , water is a mixture of both LDL and HDL phases associated with a diverging density fluctuation. At higher temperatures, the two liquid phases are indistinguishable. Lowering temperature or

---

\*All correspondence regarding this paper should be addressed to Sow-Hsin Chen (sowhsin@mit.edu).

increasing pressure will result in an increase of the LDL phase with respect to the HDL phase. The FSC can be identified by the temperature at which transport properties, like the shear viscosity  $\eta$  or the inverse self-diffusion coefficient  $1/D$ , cross over from a non-Arrhenius (fragile) to an Arrhenius (strong) behavior on approaching  $T_g$ .

A possibility to enter this inaccessible temperature range of water, named “no-man’s-land”, is now shown by confining water in nano-size pores [12, 13, 14, 15]. When contained within these pores, water does not crystallize, and can be supercooled well below  $T_H$ . Vycor pores [14, 15] (a porous hydrophilic silica glass), micellar systems or layered vermiculite clay [12] are examples of confining nano-structures. The latter systems have been used to explore the Arrhenius behavior of the dielectric relaxation time ( $\tau_D$ ) of very deeply supercooled water.

The FSC was recently confirmed by a QENS experiment, which measured the  $T$  and  $P$  dependences of the average translational relaxation time  $\langle\tau_T\rangle$  for water confined in nanopores of silica glass [16, 17]. In particular, as the temperature is lowered, a  $\langle\tau_T\rangle$  versus  $1/T$  plot exhibits a cusp-like crossover from a non-Arrhenius to an Arrhenius behavior at a temperature  $T_L(P)$ . This crossover temperature decreases steadily upon increasing  $P$ , until it intersects the  $T_H$  line of bulk water at  $P \sim 1.6$  Kbar. Beyond this point, the FSC can no longer be identified. These results, suggestive of the existence of the two liquid phases, have been explained in a molecular dynamics (MD) simulation study by considering the existence of a critical point. The MD study shows that the FSC line coincides with the line of specific heat maxima  $C_p^{\max}$ , called Widom line. The Widom line is the critical isochore above the critical point in the one-phase region [18]. Moreover, it is observed that crossing this line corresponds to a change in the  $T$  dependence of the dynamics. More precisely, the calculated water diffusion coefficient,  $D(T)$ , changes according to a FSC, while the structural and thermodynamic properties change from those of HDL to those of LDL.

## Results and Discussion

In this report, we present a detailed study done using two different experimental techniques, neutron scattering and NMR, to probe dynamical properties of confined water at low temperatures, well inside the inaccessible region of bulk water. Our main aim is to clarify the properties of water as a glass forming material, measuring directly, with NMR spectroscopy, the self diffusion coefficient  $D$  as a function of temperature, and comparing the obtained results with the translational relaxation time  $\langle\tau_T\rangle$  measured by QENS.  $\langle\tau_T\rangle$  is a quantity proportional to the viscosity  $\eta$ . These new measurements enable one to compare the proportionality of the transport coefficient  $1/D$  and viscosity  $\eta$ , and can provide a test for the theoretical description of dynamics at the molecular scale of glass forming materials. According to Ito et al.

[10], the FSC can be intimately connected to the presence of a thermodynamic event in liquid water: i.e. the temperature dependence of the inverse self-diffusion coefficient does not follow that of viscosity or inverse mutual diffusion coefficient. In other words, supercooled water must show, on approaching  $T_g$ , the marked decoupling of translational diffusion coefficient from viscosity or rotational correlation time, as recently observed in some supercooled liquids [20, 21, 22]. Here we confirm by means of NMR data the existence of a FSC in supercooled water, as proposed by the QENS and MD studies [16, 17, 18] and show, for the first time, that the Stokes-Einstein relation (SER) breaks down in different ways on both the fragile and strong sides of FSC.

Figure 1A shows a log-linear plot of the inverse of the self-diffusion coefficient of water  $1/D$  measured by NMR as a function of  $1/T$  for the fully hydrated MCM-41-S samples with pore diameters of 14 Å and 18 Å. Figure 1B reports the average translational relaxation time  $\langle\tau_T\rangle$ , obtained by analyzing QENS spectra of the same samples, versus  $1/T$ , using the Relaxing-Cage Model (RCM) as shown in Ref. [16, 17]. As it can be observed from Figure 1A and 1B, the measured values of  $D$  and  $\langle\tau_T\rangle$  are independent of the pore size of the samples. This indicates that NMR field-gradient measurements, having a length scale larger than the size of the pores, are insensitive to the system geometry. In Fig. 1A, the solid line denotes the fit of the data to a Vogel-Fulcher-Tamman (VFT) law  $1/D = 1/D_0 \exp(BT_0/(T - T_0))$ , where  $1/D_0 = 2.4 \cdot 10^7$  ( $s/m^2$ ),  $B = 1.775$ , and  $T_0 = 187$  K.  $B$  is a constant providing a measure of the system fragility and  $T_0$  the ideal glass transition temperature. The short dotted line denotes the fit to an Arrhenius law  $1/D = 1/D_0 \exp(E_A/k_B T)$ , where we keep the same  $1/D_0$  value as in the VFT law fit, and  $E_A = 3.98$  Kcal/mol. Figure 1B shows the  $\langle\tau_T\rangle$  data at ambient pressure. The dashed lines denote the VFT law fit, and the dotted lines the Arrhenius law fit, with the same pre-factor  $\tau_0$ . We obtained the following values:  $E_A = 5.4$  Kcal/mol,  $T_0 = 200$  K. The consequence of insisting on the same pre-factor in both the VFT and the Arrhenius laws results in an equation determining the crossover temperature  $T_L$  in the following form:  $1/T_L = 1/T_0 - Bk_B/E_A$ . We obtained  $T_L = 224.5$  K from the  $1/D$  data and  $T_L = 225.8$  K from the  $\langle\tau_T\rangle$  data. The agreement between NMR and QENS results is thus satisfactory, especially regarding the two relevant quantities  $E_A$  and  $T_L$ . Figure 1A and 1B also show that within the size range of 10 to 20 Å, the crossover temperature  $T_L$  is independent of pore size. As previously mentioned, a FSC occurring at 228 K has been proposed by Ito et al. [10] for water, which is fragile at room and moderately supercooled temperatures but near the glass transition temperature it is shown to be a strong liquid by dielectric relaxation measurements [12]. The interpretation of this transition as a variant of the structural arrest transition (as predicted by the ideal mode coupling theory) was the essence of the recent QENS study of the structural

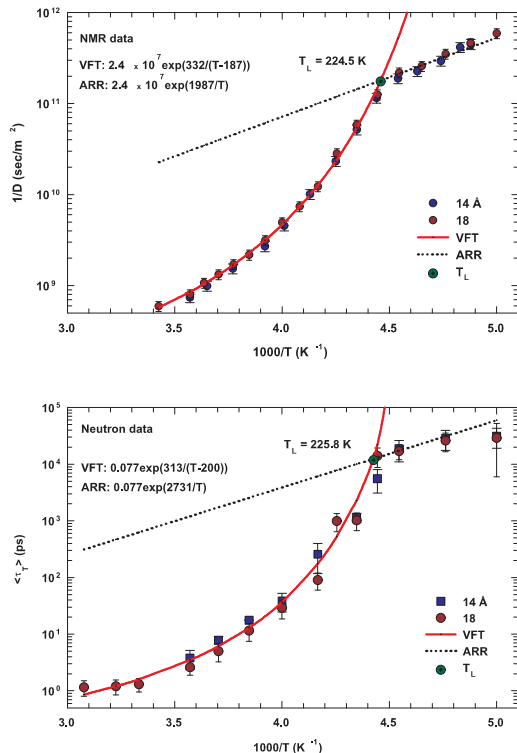


FIG. 1: Figure 1A shows, for the fully hydrated MCM-41-S samples with diameter 14 Å and 18 Å, the inverse of the self-diffusion coefficient of water  $D$  measured by NMR as a function of  $1/T$  in a log-linear scale. The solid line denotes the fit of the data to a Vogel-Fulcher-Tamman (VFT) relation. The short dotted line denotes the fit to an Arrhenius law with the same prefactor  $1/D_0$ . Figure 1B reports, as a function of  $1/T$ , the average translational relaxation time  $\langle \tau_T \rangle$  obtained from QENS spectra in the same experimental conditions of the NMR experiment. The dashed line denotes the VFT fit, and the dotted line the Arrhenius law fit with the same prefactor  $\tau_0$ . In both panels, the values of fitting parameters are shown.

relaxation time and MD study of the self-diffusion coefficient [16, 17, 18]. These NMR results presented above constitute, by means of a direct measurement of the self-diffusion coefficient of supercooled water, an independent confirmation of the existence of FSC in water.

Let us now focus on the SER that relates the self-diffusion coefficient  $D$ , viscosity  $\eta$ , and temperature  $T$  as  $D \propto T/\eta$ , which, as it is well known, is usually accurate for normal and high temperature liquids. Since  $\langle \tau_T \rangle$  is proportional to the viscosity, we examine the relationship between  $D$  and  $\langle \tau_T \rangle$  in figure 2. In this figure the quantity  $D \langle \tau_T \rangle / T$  is reported as a function of  $T$ . Dots and squares represent its values coming from the experimen-

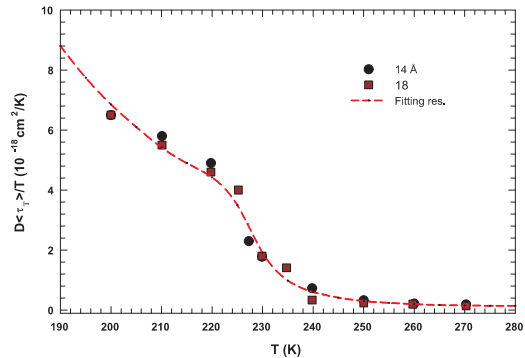


FIG. 2: The figure reports the quantity  $D \langle \tau_T \rangle / T$  as a function of  $T$ . Dots and squares represent its values coming from the experimental data of  $D$  and  $\langle \tau_T \rangle$  in samples with diameter 14 Å and 18 Å, respectively. The dotted line represents same quantity obtained by using the fitting values obtained from the data reported in Fig 1A and 1B.

tal data of samples with pore diameters of 14 and 18 Å, respectively, whereas the dotted line represents the same quantity obtained using the corresponding fitted lines reported in figure 1A and 1B. The temperature dependence of  $D \langle \tau_T \rangle / T$  shows that this quantity is constant at higher  $T$ , but increases steeply as  $T$  goes below the FSC temperature. Furthermore, it shows a small bump at the FSC temperature, in accordance with the predictions of a recent theoretical study [19]. Therefore, in the supercooled region the temperature behavior of  $D$  and  $\langle \tau_T \rangle$  is inconsistent with SER, signalling a marked decoupling between these two transport parameters, on decreasing  $T$ . In recent experimental studies on some supercooled liquids, it has been reported that SER breaks down as the glass transition is approached. The self-diffusion coefficient shows, as far as water in the present experiment is concerned, an enhancement of orders of magnitude from what expected from SER [20, 21, 22, 23, 24]. These decouplings of the transport coefficients, observed as a SER violation, have been attributed to the occurrence of dynamical heterogeneities in structural glass formers [20, 22, 25, 26]. Thus, in supercooled liquids there exist regions of varying dynamics, i.e. fluctuations that dominate their transport properties near the glass transition. The extent of such decouplings may depend on the material and the microscopic details of the specific transport parameters.

The SER breakdown can be described using a scaling concept, in particular, the law  $D \sim \tau^{-\xi}$ , where  $\xi = \alpha(T)/\beta(T)$  with  $\alpha$  and  $\beta$  being temperature dependent scaling exponents of  $D$  and  $\tau$ , respectively [27]. Recently, it has been shown that for tris-naphthylbenzene (a fragile glass former)  $\xi = 0.77$  [22], whereas an MD simulation of Lennard-Jones binary mixture has given

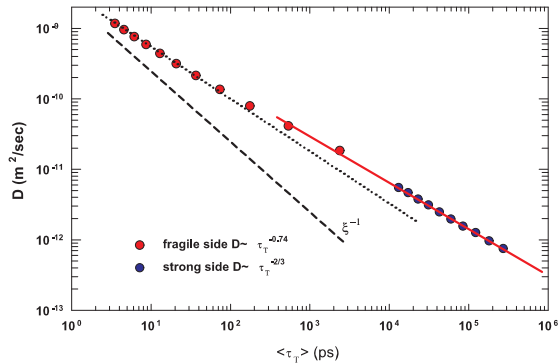


FIG. 3: The scaling plot in a log-log scale of  $D$  vs  $\langle\tau_T\rangle$ . Red dots are data corresponding to temperatures above  $T_L$ , i.e. when water is in the fragile glass phase, whereas blue dots correspond to the strong Arrhenius region. Two different scaling behaviors exist above and below the temperature of the FST. In the fragile region the scaling exponent is  $\xi \simeq 0.74$  (dotted line) and  $\sim 2/3$  in the strong side (solid line). Dashed line represents the situation in which the SER holds,  $D \sim \tau^{-1}$ .

$\xi = 0.75$  [28]. By using such an approach, we will discuss our SER results for confined supercooled water. Figure 3 shows the  $D$  vs  $\langle\tau_T\rangle$  plot in a log-log scale. The red dots represent data corresponding to temperatures above  $T_L$ , where water behaves as a fragile glass former, and the blue dots pertain to the strong Arrhenius region. As it can be observed, the data clearly show two different scaling behaviors above and below the FSC temperature, in particular  $\xi \simeq 0.74$  on the fragile side (dotted line) and  $\sim 2/3$  on the strong side (solid line). Dashed line represents the situation in which SER holds,  $D \sim \tau^{-1}$ . These results agree with those obtained in tris-naphthylbenzene [22] and, more specifically, with those of a recent theoretical study in which the decoupling of transport coefficients in supercooled liquids was investigated by using two class of models, one describing diffusion in a strong glass former, and the other in a fragile one [27]. The main result of this study is that, while in the fragile case the SER violation is weakly dependent on the dimensionality  $d$ , with  $\xi = 0.73$ , in the strong case the violation is sensitive to  $d$ , going as  $D \sim \tau^{-2/3}$  for  $d = 1$ , and as  $D \sim \tau^{-0.95}$  for  $d = 3$ . On considering the geometry of the system that we have used in our experiment to confine water (1D cylindrical tubes, with a length of some  $\mu m$  and pore diameters of 14 Å and 18 Å), the scaling plot shown in Figure 3 compares remarkably well with the findings of the theoretical investigation [27], on both fragile and strong sides.

In summary, we explore dynamical properties of water in a deeply supercooled regime (well inside the “no-man’s land”) by means of NMR and QENS experiments, which separately give a conclusive proof of the existence of a

FSC. This supports the hypothesis that liquid water is consisting of a mixture of two different liquid structures (the LDL and HDL phases). Accordingly, a liquid-liquid phase separation line exists in the  $P - T$  plane with a liquid-liquid critical point as its end point. Remarkably, we give the first experimental proof of the existence of a violation of SER above and below the FSC in water, i.e. in both the fragile and strong regimes of supercooled water. This clearly reflects the decoupling of transport coefficients of the liquid when temperature is lowered toward  $T_g$ . This latter result certainly constitutes a new element which serves to clarify one of the most intriguing properties of water.

## Methods

Water was confined in micellar templated mesoporous silica matrices MCM-41-S, which have 1-D cylindrical pores with a length of some  $\mu m$  arranged in 2-D hexagonal arrays, synthesized following a similar method for the previous synthesis of MCM-48-S [29]. The MCM-41-S materials are the same as those previously used in the QENS study of confined water [17]. Pore size was determined using nitrogen absorption-desorption technique [16, 17]. Investigated samples have hydration levels of  $H \simeq 0.5$  (0.5 gram  $H_2O$  per gram of MCM-41-S), obtained by exposing dry powder samples to water vapor at room temperature in a closed chamber. This water confining system can be regarded as one of the most suitable adsorbent models currently available [30, 31].

High-resolution QENS spectroscopy method was used to determine the temperature dependence of  $\langle\tau_T\rangle$  for confined water. Because neutrons can easily penetrate the wall of sample cell and because they are predominantly scattered by hydrogen atoms in water, rather than by the matrices containing them, incoherent QENS is an appropriate tool for our study. Using two separate high-resolution QENS spectrometers, we were able to measure the translational-relaxation time from 0.2 ps to 10,000 ps over the whole temperature range under study. The experiments were performed at both the High-Flux Backscattering (HFBS) and the Disc-Chopper Time-of-Flight (DCS) spectrometers in the NIST Center for Neutron Research (NIST NCNR). The two spectrometers have two widely different dynamic ranges (for the chosen experimental setup), one with an energy resolution of 0.8  $\mu eV$  (HFBS) and a dynamic range of  $\pm 11 \mu eV$  [32], and the other with an energy resolution of 20  $\mu eV$  (DCS) and a dynamic range of  $\pm 0.5 meV$  [33] in order to be able to extract the broad range of relaxation times from the measured spectra. The experiment was done at a series of temperatures, covering both below and above the transition temperature, and the data were analyzed using Relaxing-Cage Model to extract the average translational relaxation time  $\langle\tau_T\rangle$ .

The NMR experiments on fully hydrated MCM-41-S samples with pore diameters of 18 and 14 Å, were per-

formed at ambient pressure using a Bruker AVANCE NMR spectrometer, operating at 700 MHz proton resonance frequency. The self-diffusion coefficient of water  $D$  was measured with the pulsed gradient spin-echo technique (PGSE) [34, 35], in the temperature range 190 K - 298 K (with an accuracy of  $\pm 0.2$  K). The  $T$  dependence of the chemical shift of methanol was used as a  $T$  standard. All details about the NMR experiment and the sample properties are reported elsewhere [36]. The reported  $D$  values were derived from the measured mean square displacement  $\langle r^2(t) \rangle$  of molecules diffusing along the NMR pulsed field gradients direction  $\mathbf{r}$ , during the time interval  $t$ .

### Acknowledgements

Authors would like to thank Chun-Wan Yen from National Taiwan University for preparing MCM-41-S sam-

ples. Technical supports in QENS measurements from E. Mamontov and J.R.D. Copley at NIST NCNR are greatly appreciated. The research at MIT is supported by DOE Grants DE-FG02-90ER45429 and 2113-MIT-DOE-591. The research in Messina is supported by the MURST-PRIN2004. This work utilized facilities supported in part by the National Science Foundation under Agreement No. DMR-0086210. The work utilized facilities of the Messina SCM-HR-NMR Center of CNR-INFM. We benefited from affiliation with EU Marie-Curie Research and Training Network on Arrested Matter.

- 
- [1] Angell, C.A. (1982) in *Water: a Comprehensive Treatise Vol.7*, ed. Franks, F. (Plenum, New York) 1-81.
- [2] Debenedetti, P.G. & Stanley, H.E. (2003) *Physics Today* **56**, 40-46.
- [3] Mishima, O. & Stanley, H.E. (1998) *Nature*, **396**, 329-335.
- [4] Velikov, V., Borick, S. & Angell, C.A. (2001) *Science*, **294**, 2335-2338.
- [5] Sokolov, A. P. (1996) *Science* **273**, 1675-1676.
- [6] Götze, W. & Sjölander, L. (1992) *Rep. Prog. Phys.* **55**, 241-376.
- [7] Angell, C.A. (1997) in *Complex Behavior of Glassy Systems*, Rubí, M. & Péres-Vicente, C. (Springer, Berlin).
- [8] Angell, C.A. (1995) *Science* **267**, 1924-1935.
- [9] Poole, P.H., Sciortino, F., Essmann, U. & Stanley, H.E. (1992) *Nature* **360**, 324-328.
- [10] Ito, K., Moynihan, C.T. & Angell, C.A. (1999) *Nature* **398**, 492-495.
- [11] Soper, A.K. & Ricci, M.A. (2000) *Phys. Rev. Lett.* **84**, 2881-2884.
- [12] Bergman, R. & Swenson, J. (2000) *Nature* **403**, 283-286.
- [13] Koga, K., Tanaka, H. & Zeng, X.C. (2000) *Nature* **408**, 564-567.
- [14] Webber, B. & Dore, J. (2004) *J. of Phys. Cond. Matt.* **16**, S5449-S5470.
- [15] Dore, J. (2000) *Chem. Phys.* **258**, 327-347.
- [16] Faraone, A., Liu, L., Mou, C.-Y., Yen, C.-W. & Chen, S.-H. (2004) *J. Chem. Phys.* **121**, 10843-10846.
- [17] Liu, L., Chen, S.-H., Faraone, A., Yen, C.-W. & Mou, C.-Y. (2005) *Phys. Rev. Lett.* **95**, 117802-1-117802-4.
- [18] Xu, L., Kumar, P., S. Buldyrev, V., Chen, S.-H., Poole, P. H., Sciortino, F. & Stanley, H. E. (2005) *Proc. Natl. Acad. Sci. USA* **102**, 16558-16562.
- [19] Pan, A.C., Garrahan, J.P. & Chandler, D. (2005) *Chem. Phys. Chem.* **6**, 1783-1785.
- [20] Ediger, M. D. (2000) *Ann. Rev. Phys. Chem.* **51**, 99-128.
- [21] Fujara, F., Geil, B., Sillescu, H. & Fleishcer, G. (1992) *Z. Phys. B* **88**, 195-204.
- [22] Swallen, S. F., Bonvallet, P.A., McMahan, R. J. & Ediger, M.D. (2003) *Phys. Rev. Lett.* **90**, 015901-1-015901-4.
- [23] Chang, J. & Sillescu, H. (1997) *J. Phys. Chem. B.* **101**, 8794-8801.
- [24] Cicerone, M.T. & Ediger, M.D. (1996) *J. Chem. Phys.* **104**, 7210-7218.
- [25] Xia, X.Y. & Wolynes, P.G. (2001) *J. Phys. Chem. B* **105**, 6570-6573.
- [26] Ngai, K.L., Magill, J.H. & Plazek, D.J. (2000) *J. Chem. Phys.* **112** 1887-1892.
- [27] Jung, Y.-J., Garrahan, J. P. & Chandler, D. (2004) *Phys. Rev. E* **69**, 061205-1-061205-7.
- [28] Yamamoto, R. & Onuki, A. (1998) *Phys. Rev. Lett.* **81**, 4915-4918.
- [29] Shih, P.-C., Lin, H.-P., & Mou, C.-Y. (2003) *Stud. Surf. Sci. Catal.* **146**, 557-560.
- [30] Schreiber, A., Ketelsen, I. & Findenegg, G.H. (2001) *Phys. Chem. Chem. Phys.* **3**, 1185-1195.
- [31] Morishige, K. & Nobuoka, K. (1997) *J. Chem. Phys.* **107**, 6965-6969.
- [32] Meyer, A., Dimeo, R.M., Gehring, P.M., & Neumann, D.A. (2003) *Rev. Sci. Instrum.* **74**, 2759-2777.
- [33] Copley, J.R.D. & Cook, J.C. (2003) *Chem. Phys.* **292**, 477-485.
- [34] Stejskal, E.O. & Tanner, J.E. (1965) *J. Chem. Phys.* **42**, 288-292.
- [35] Price, W.S. (1998) *Concepts Mag. Reson.* **10**, 197-237.
- [36] Mallamace, F., Broccio, M., Corsaro, C., Faraone, A., Wanderlingh, U., Liu, L., Mou, C.-Y. & Chen, S.-H. (2006) *J. Chem. Phys.*, in press.